JOURNAL OF MATERIALS SCIENCE 30 (1995) 4507–4514

Thermophysical properties of ceramic matrix composites produced by polymer pyrolysis

P. J. GOULD, A. BOHNERT*, R. J. DAY, R. TAYLOR
Manchester Materials Science Centre, Grosvenor Street, Manchester M1 7HS UK

A unidirectional composite and a series of bidirectionally reinforced composites were fabricated using carbon fibre reinforcement in a silicon carbide matrix, which was produced by the pyrolysis of a polymer precursor. The thermal expansion over the temperature range 20–1000 °C has been measured and the thermal diffusivity measured over the temperature range 200–1200 °C. Thermal diffusivity data was converted to conductivity data using measured density and literature specific heat data. Metallographic examination has been carried out on the composites and the results are discussed in terms of the observed microstructural features.

1. Introduction

Ceramic matrix composites have great potential for use in high temperature applications and successful composites are made by impregnating an orthogonal fibre array with a matrix of carbon or silicon carbide, deposited by chemical vapour deposition (CVD) [1]. The major barriers to more widespread use of these composites are the long production times and their high production costs. If ceramic matrix composites are to find more widespread markets then new, more cost-effective, methods of production have to be found. One potentially attractive route is via polymer pyrolysis where the fibre reinforcement is infiltrated with a ceramic-precursor polymer. Such polymers are based upon a backbone chain comprising silicon atoms or alternating silicon and carbon atoms, and they are produced with a variety of side chains which govern the properties of the polymer and its subsequent ceramic yield. Polymers that are liquid at room temperature can be used for infiltration without further processing whereas those that are solid need to be dissolved prior to infiltration. A short curing heat treatment to ca. 300 °C in air renders the green composite infusible by cross-linking the polymer chains and a subsequent pyrolysis heat treatment to ca. 1000 °C in inert atmosphere converts the polymer to ceramic [2].

For ceramic matrix composites that are to be used in high temperature applications, it is important to know their thermophysical properties as a function of temperature so that the service behaviour of components made from such materials can be predicted. Composite properties will be strongly influenced by the micro- and macrostructural features of the composites. These in turn will be dependent both on the processing route used and the variation in processing parameters. This study examines the thermal diffusivity and thermal expansion of carbon-fibre-reinforced silicon carbide produced by a polymer pyrolysis route [3], and seeks to relate the properties measured with the microstructure of the composites.

The thermophysical properties of a range of orthogonally reinforced composites have been measured by a number of workers and these have been reviewed by Mottram and Taylor [4]. Whittaker *et al.* [5] measured the thermal transport properties of carbon/carbon fibre composites from 300 to 3000 K. Relatively few measurements have been undertaken on ceramic matrix composites. Tawil *et al.* [6] used the laser flash technique to measure the thermal diffusivity of SiC- or carbon-fibre-reinforced SiC matrix composites produced by CVD. Measurements on similar materials were reported by Taylor *et al.* [7]. In each case the reinforcement was Nicalon fibres. Izawa *et al.* [8] and Scafè *et al.* [9] have both measured the room temperature expansion coefficient and thermal conductivity of a silicon/silicon carbide composite constructed by reacting molten silicon with graphite. Results have been reported by Wang *et al.* [10] on carbon/silicon carbide composites. They produced a whole range of carbon/silicon carbide ratios by chemical vapour deposition and measured the thermal conductivity of these composites in the temperature range from room temperature to 1200 K. They also measured the thermal expansion of the composites to 900 K. The only measurements on composites with a matrix made by the polymer–pyrolysis route are those by Semen and Loop [11] on SiC powder/Si_3N_4 composites where the Si_3N_4 matrix was formed from pyrolysis of a polysilazane precursor.

2. Experimental Procedure

The composites examined in this study were unidirectional and bidirectional layups of sheets of

Present address: HAB-Weimar, Weimar, Germany.

0022–2461

filament-wound carbon fibre in a silicon carbide matrix produced by Dornier GmbH [3]. The thicknesses of these varied from eight to 15 layers, i.e. from 2.5 to 5 mm thick with the layups for the bidirectional composites alternating. 0°/90°/0°/90°/90°/0°/90°/0°. The fibre tows were impregnated with a slurry of silicon carbide powder in liquid precursor polymer. The composites were laid up in the green state, cured and then subjected to a pyrolysis heat treatment to convert the polymer to silicon carbide. A table of the different materials with their designations is given in Table I. Some of the composites were re-impregnated several times in order to increase their final density, each impregnation with liquid precursor being followed by a pyrolysis heat treatment; three infiltrations thus means pyrolysed in the prepreg stage followed by three further infiltrations of liquid precursor.

Cuboids of materials ca. 10 mm long were cut from the composite using a diamond wafering blade and were trimmed by grinding to ensure that, as measured using a ball micrometer, their ends were parallel within a few micrometres. The thermal expansion measurements were to be carried out in argon atmosphere but this would still contain oxygen as an impurity and the experimental times were long. Thus, in order to avoid degradation of the carbon fibres through oxidation, a gold coating of a few tens of nanometres was given to the composites for additional protection. Gold was used as the most readily available thin coating material and such a thin layer should have no effect on the expansion measured.

For the thermal expansion experiments the samples were placed individually in a vertically mounted alumina pushrod dilatometer. The dilatometer used a linear variable differential transducer to detect the changes in length with the sample placed between the recrystallized alumina pushrod and the flat end of the recrystallized alumina containment tube. A run without a sample was carried out first in order to calibrate the expansion of the tube and pushrod assembly. The thermal expansion was measured only in the plane direction parallel to one of the fibre directions for the 2D layup composites but in two directions, parallel and perpendicular to the fibre axes, for the unidirectional layup composite.

The heating and cooling cycles used for each sample were identical, comprising a heating ramp of 1 °C min^{-1} from room temperature to 1000 °C followed immediately by a cooling ramp to room temperature at the same rate. This slow heating/cooling rate was used so that thermal equilibrium could be reached in the sample. The data sets of expansion against temperature were then corrected for system effects, point by point, using the data from the run without a sample.

The thermal diffusivities of the samples were measured in vacuum using the laser flash technique [12]. In this technique one face of a thin piece of the material is subjected to a heat pulse supplied by a laser. The transient temperature rise of the other face is measured and the time for the temperature to reach half of its maximum value, $t_{1/2}$, is determined. This half-rise time, together with the thickness of the sample, L, and a dimensionless heat term, ω/π^2, give the diffusivity of the material using Equation 1

$$\alpha = \frac{(\omega/\pi^2)L^2}{t_{1/2}} \quad (1)$$

TABLE I Specimen details for the composites studied

	Layup	Production details
UM1	1D	Three infiltrations
UM2	2D	Three infiltrations
UM3	2D	Three infiltrations
UM4	2D	Pyrolysed prepreg, no further infiltrations
UM5	2D	Pyrolysed prepreg, no further infiltrations

The apparatus used [13] comprised: a 100 J Nd/glass laser with a wavelength of 1.067 μm and a pulse dissipation time of 0.6 ms; a calcium fluoride lens and mirror system to focus the radiation from the back face onto an InSb infrared detector; an induction coil to heat the graphite susceptor that contained the sample in its graphite holder. The whole was enclosed in a containment vessel that could be evacuated or filled with inert gas.

The unidirectional layup composite was again measured in directions parallel and perpendicular to the fibre axes, whereas the bidirectional composites were measured in directions parallel and perpendicular to the plane of the fibre layup. When measured perpendicular to the layup planes the samples had to contain at least three fibre layers in order to ensure a homogeneous medium response for the composite for which fibre and matrix conductivities could be markedly different [14, 15]. Densities of the composites were measured using the Archimedean displacement method and the specific heats of the composites were calculated using a weighted mean of the standard values for silicon carbide and graphite. Microstructural analysis was carried out by light microscopy. Sections of the composite were cut using a high speed diamond saw and were polished to a 1 μm diamond finish prior to examination. The volume fractions of fibre and porosity in the matrix were measured using image analysis. This was carried out using an Olympus BH2 microscope in conjunction with the GENIAS v4.6 image analysis software.

3. Results

The thermal expansion results for sample UM1 in the longitudinal and transverse directions are shown in Fig. 1. The thermal expansion measured in the longitudinal direction is significantly higher than that measured in the transverse direction and, significantly, both curves exhibit very little hysteresis. Both curves also show a change in slope at ca. 600 °C, with the most noticeable change being shown by the transverse curve for which the thermal expansion changes from almost zero to a slight positive value.

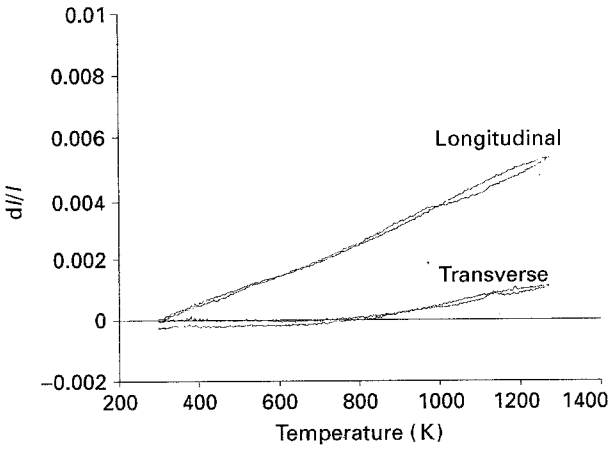

Figure 1 Thermal expansion of UM1.

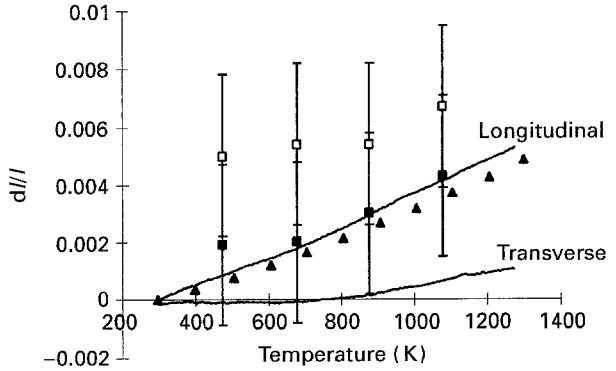

Figure 2 Thermal expansion of UM1 compared with the thermal expansion of its components. —, Composite; ▲, SiC; □, C fibre radial; ■, C fibre axial.

The lack of hysteresis allows the point-by-point average of the heating and cooling curves to be taken and this average is displayed in Fig. 2, where it is compared with reference book data for SiC [16] and literature data for the axial and radial thermal expansion of T300 carbon fibre deduced from transmission electron microscope observations of the change in dimensions of the fibre when heated [17]. No data was available for T800 fibres but the two fibres are produced by the same manufacturer and have similar microstructures so use of T300 data seems justifiable.

In the longitudinal direction of the composite, the measured expansion curve closely follows the reference book data for silicon carbide, whereas the thermal expansion of the axial carbon fibre is much higher and a different shape. As the composite has a large proportion of fibres and matches the silicon carbide expansion to within 10%, it would appear that the carbon fibres do not make a significant contribution to the thermal expansion of the composite in this direction.

The transverse expansion curve shows very little overall expansion regardless of the fact that the radial expansion of carbon fibres is higher than the expansion of silicon carbide. Clearly the fact that the composite expansion is nominally zero up to

TABLE II Coefficients of thermal expansion for the unidirectional composite

	Linear coefficient of thermal expansion (K^{-1})
Longitudinal	$6.36 \pm 0.04 \times 10^{-6}$
Transverse	$2.45 \pm 0.03 \times 10^{-6}$

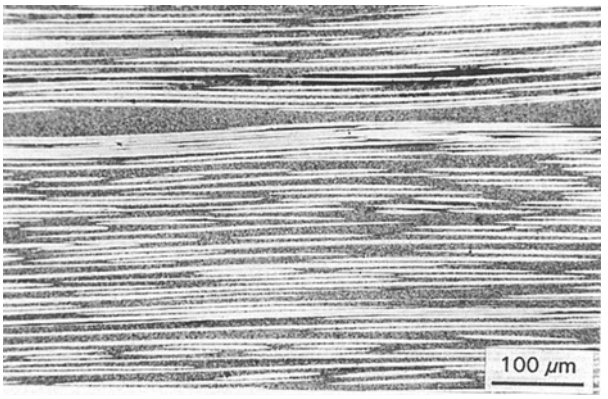

Figure 3 Light micrograph of a longitudinal section of UM1.

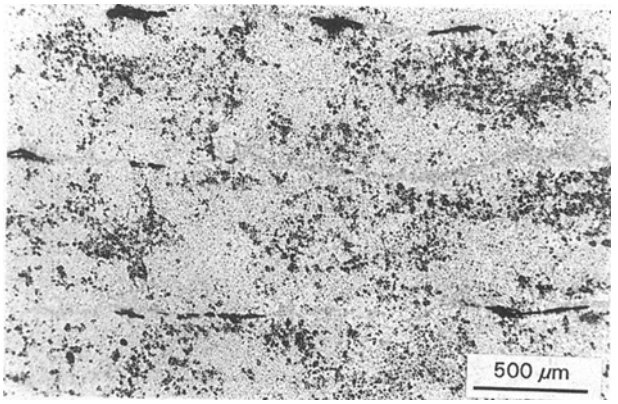

Figure 4 Light micrograph of a transverse section of UM1.

500 °C suggests that all expansion of matrix and fibre is completely taken up by the porosity present. The porosity is due mainly to interfacial voids and shrinkage of the matrix when the polymer is pyrolysed, but also partly due to microcracking on cooling from the processing temperature. The change in slope between 500 and 600 °C to a finite positive value indicates that some, but not all, of the porosity is squeezed shut. The slope of the transverse expansion never reaches that of the longitudinal expansion curve nor that of silicon carbide. This change in slope can also be seen in the longitudinal expansion curve.

Fitting the portions of the two curves to a straight line above 600 °C gives values for the linear coefficient of thermal expansion in each direction (Table II).

Light micrographs of polished sections of the UM1 composite in the longitudinal and transverse directions are given in Figs 3 and 4. The longitudinal section appears dense, exhibiting little porosity and no matrix cracking. The transverse section shows rather more porosity including some elongated porosity at the interfaces between fibre tows. Image analysis gives

the volume fractions of porosity and fibre to be 12 and 54%, respectively.

A variety of mathematical models have been developed to predict the thermal expansion of aligned fibre composites. These models have been reviewed by a number of authors [18, 19], and most of the treatments are based on the assumptions that perfect adhesion exists between fibre and matrix and the porosity levels are small. These models, which predict that the composite expansivity is intermediate between fibre and matrix, have been used with varying levels of success, mainly with polymer–matrix composites. For carbon fibre/silicon carbide matrix composites which have been fabricated at much higher temperatures, the assumptions of perfect interfacial contact and low porosity levels are unlikely to be valid.

Yates *et al.* [20] successfully used the following equation

$$\alpha_c = \frac{E_m V_m \alpha_m + E_f^{\parallel} V_f \alpha_f^{\parallel}}{E_m V_m + E_f^{\parallel} V_f} \quad (2)$$

to explain the axial thermal expansivity of unidirectional carbon-fibre-reinforced polymer matrix composites although, as noted by Schapery [21], this simple equation is only valid if the Poisson's ratio for the two components are the same. Here, E is Young's modulus, V is the volume fraction, α is the thermal expansion coefficient, the subscript m refers to matrix and the subscript f and superscript $\parallel$ refer to the carbon fibre parallel to the fibre axis. The Poisson's ratio for the carbon fibre is 0.22 [17] and that for the matrix 0.18 [22], so Equation 2 may not be entirely valid. Using values of: $E_m = 410$ GPa [22]; $E_f = 300$ GPa [23]; $\alpha_m = 4.3 \times 10^{-6}\ K^{-1}$ [22]; $\alpha_f = 4.5 \pm 5 \times 10^{-6}\ K^{-1}$ [17] for these parameters, Equation 2 yields a theoretical value of the composite expansion coefficient in the longitudinal direction of $4.4 \pm 6 \times 10^{-6}\ K^{-1}$. The large error is entirely due to the uncertainty in the longitudinal expansion coefficient of the carbon fibre.

Clearly, any attempt to compare the transverse thermal expansion with existing models would be pointless because of the high porosity levels. Undoubtedly, the low, almost zero, expansion coefficient noted on heating up to 600 °C is due to the fact that the solid expansion is filling the porosity which is in the form of cracks in the composite.

The other four samples are all 0°/90° layups and should have in-plane thermal expansions that reflect the 0 and 90° fibre orientations in alternate layers; ideally, an average of the axial and transverse thermal expansions of the unidirectional composite UM1. The expansion curves for samples UM2–5 are shown in Figs 5–8. Features similar to those observed in the unidirectional composite are noted, namely that there is a change in slope above 400 °C. Linear coefficients of thermal expansion for the higher temperature part of the curve are listed in Table III.

However, real variations may be noted in the appearance of the curves. The curve that is most similar to that exhibited in the longitudinal direction of

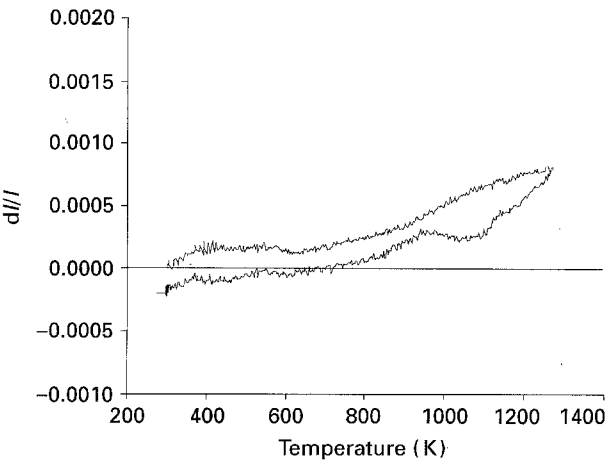

Figure 5 Thermal expansion of UM2.

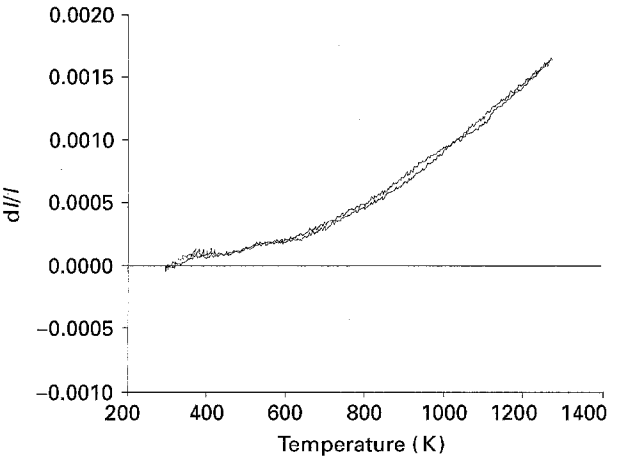

Figure 6 Thermal expansion of UM3.

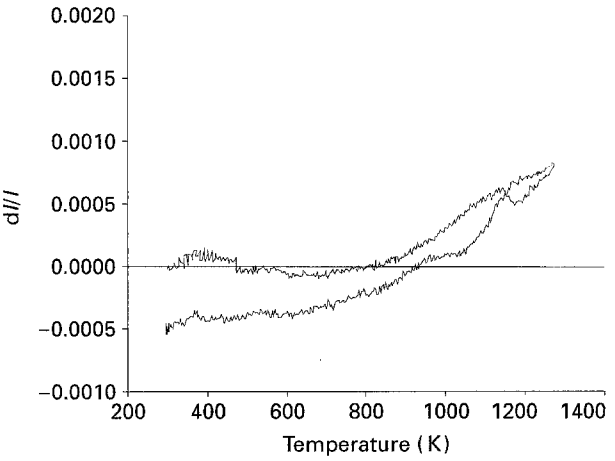

Figure 7 Thermal expansion of UM4.

sample UM1 is exhibited by sample UM3. This shows very little hysteresis and, although it does not exhibit the highest expansion coefficient, results in the largest total expansion of the 2D composites. The other three samples show significant hysteresis and a lower level expansion. Samples UM2 and UM4 show large deviations from the heating curve on cooling to 600 °C. It is also worth noting that the final total contractions for samples UM4 and UM5 are almost identical. With the exception of sample UM2, the values for the

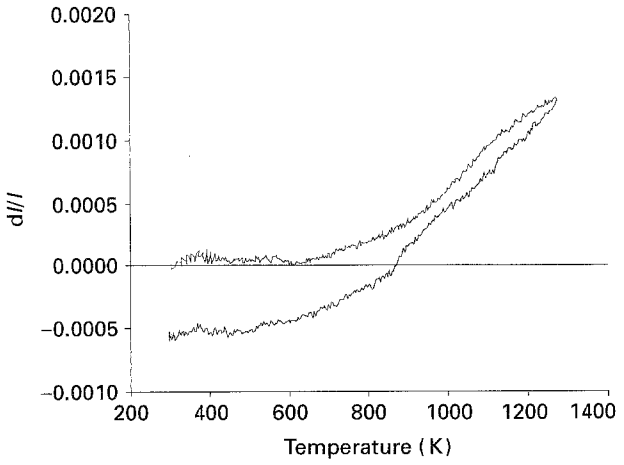

Figure 8 Thermal expansion of UM5.

TABLE III Coefficients of thermal expansion for the bidirectional composites

	Linear coefficient of thermal expansion (K^{-1})
UM2	$1.0 \pm 0.05 \times 10^{-6}$
UM3	$2.58 \pm 0.01 \times 10^{-6}$
UM4	$2.0 \pm 0.02 \times 10^{-6}$
UM5	$2.76 \pm 0.04 \times 10^{-6}$

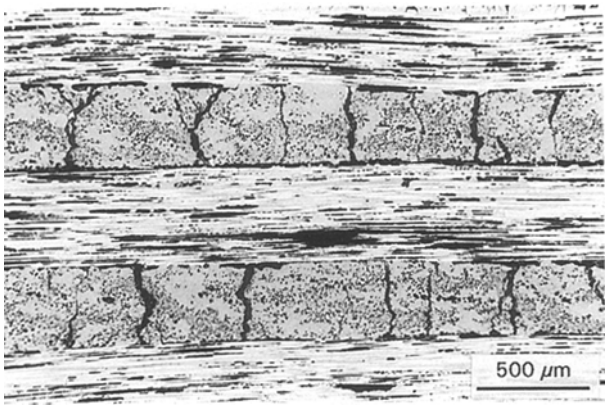

Figure 9 Light micrograph of a transverse section of UM2.

expansion coefficients given in Table III are broadly similar to the transverse expansion coefficient of the unidirectional composite. This would imply that the expansion of the bidirectional composites is being dominated by the transverse layers.

Light micrographs of polished transverse sections of samples UM2–5 are given in Figs 9–12. It can be seen from these that there is a large amount of transverse cracking together with substantial porosity in all of the composites. As expected, the most dense composites are those that have had multiple impregnations: i.e. samples UM2 and UM3. Image analysis results for the volume fractions of porosity and fibre are given in Table IV.

Clearly, the cracks, caused by shrinkage during the pyrolysis of the precursor polymer and thermal expansion mismatch on cooling from the production temperature, run mainly transversely to the direction of

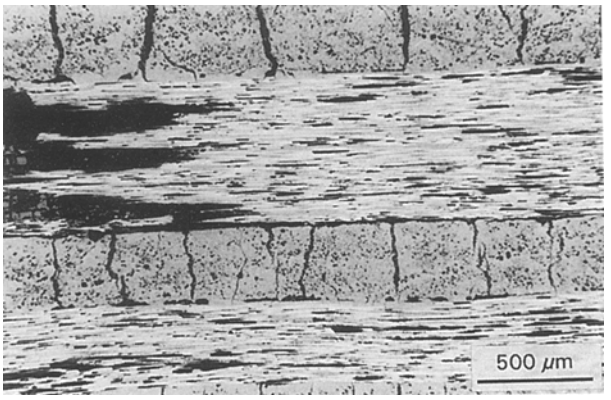

Figure 10 Light micrograph of a transverse section of UM3.

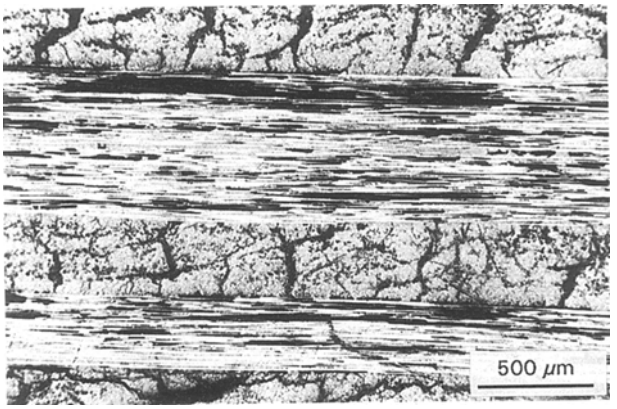

Figure 11 Light micrograph of a transverse section of UM4.

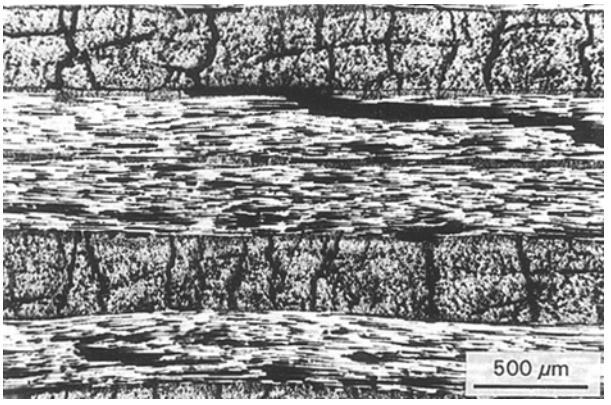

Figure 12 Light micrograph of a transverse section of UM5.

TABLE IV Volume fractions and porosity levels in the bidirectional composites

Sample	Porosity (%)	Fibre volume fraction (%)
UM2	21	48
UM3	24	47
UM4	31	45
UM5	30	42

the expansion and will substantially lower the measured thermal expansion until they have closed. It would be expected from the porosity results that sample UM2 should have a higher expansion than

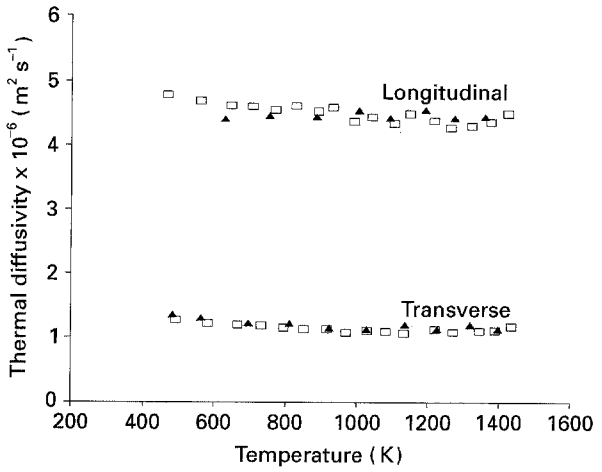

Figure 13 Thermal diffusivity data for UM1. □, Heating; ▲, cooling.

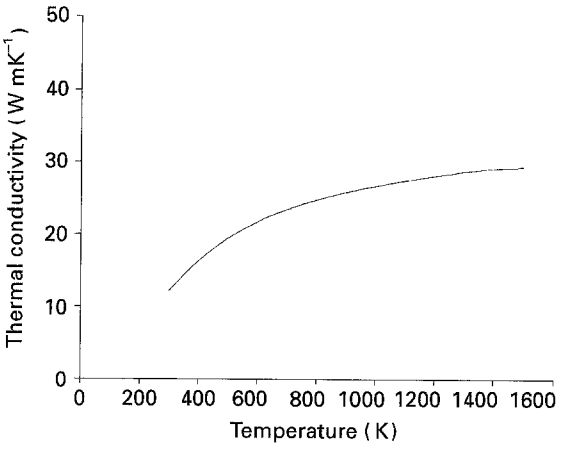

Figure 15 Thermal conductivity of the composite matrix derived using Equation 6.

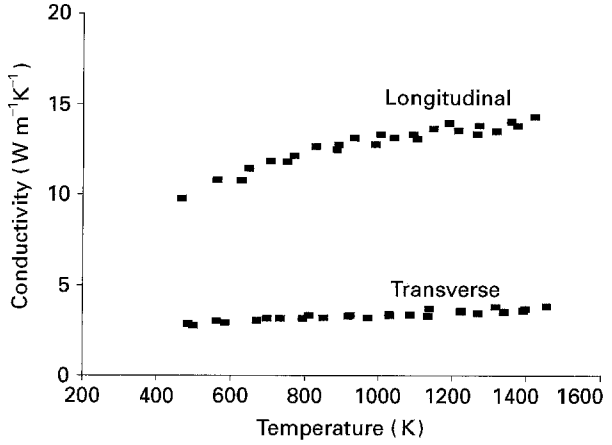

Figure 14 Thermal conductivity of UM1 derived using Equation 3.

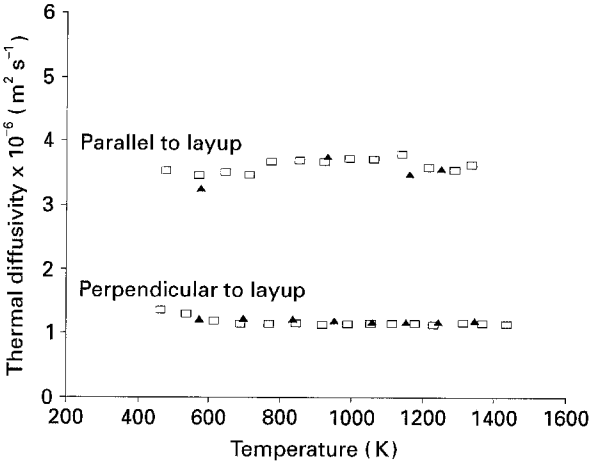

Figure 16 Thermal diffusivity data for UM2. □, Heating; ▲, cooling.

UM3, having a lower porosity level. The differences between sample UM3 and samples UM4 and UM5 can be explained by the larger amount of porosity and cracking leading to a lower initial expansion and a lower total expansion. The fact that UM2 is similar to UM4 and UM5, whilst having a lower porosity level than UM3, is anomalous and suggests that the detailed microstructures and geometry of the porosity are important in governing the thermal expansion of 2D composites.

The thermal diffusivity results for the unidirectional composite, sample UM1, are shown in Fig. 13. The composite shows a roughly consistent diffusivity over the whole temperature range in both longitudinal and transverse directions. Parallel to the fibre axis the average thermal diffusivity was $4.5 \times 10^{-6}\ m^2\ s^{-1}$, whereas normal to the fibre axis the average thermal diffusivity was $1.2 \times 10^{-6}\ m^2\ s^{-1}$. Negligible hysteresis was noted between the heating and cooling curves. The measured diffusivity (α_c) can be converted to thermal conductivity (λ_c) (Fig. 14) using the following equation

$$\lambda_c = \alpha_c(\rho_f V_f C_f + \rho_m V_m C_m) \quad (3)$$

where ρ_f and ρ_m are the densities of the fibre and matrix, and C_f and C_m the specific heats of fibre and matrix [24], respectively. The specific heats of the fibre and matrix are given as polynomials by Touloukian and Buyco [25]

$$C_{p(fibre)} = -683 + 5.9199T - 5.5271 \times 10^{-3}T^2 + 2.6677 \times 10^{-6}T^3 - 6.4429 \times 10^{-10}T^4 + 6.1622 \times 10^{-14}T^5 \quad (4)$$

$$C_{p(SiC)} = -1263.208 + 11.7869T - 0.0242T^2 + 2.495 \times 10^{-5}T^3 - 1.2547 \times 10^{-8}T^4 + 2.4549 \times 10^{-12}T^5 \quad (5)$$

The conductivity of the composite in the direction parallel to the fibre axes is given by the series model of heat conduction [26]

$$\lambda_c = V_m\lambda_m + V_f\lambda_f \quad (6)$$

where V_m and V_f are the volume fractions of matrix and fibre, respectively, and λ_m and λ_f their respective conductivities. The volume fractions are obtained from image analysis of the polished sections of the composites, Table IV. Using conductivity data for T800 fibres of Taylor *et al.* [26], the conductivity of the composite matrix may be deduced; this is shown in Fig. 15.

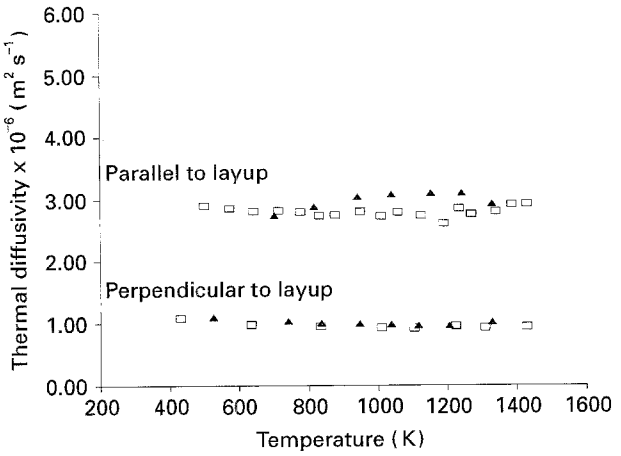

Figure 17 Thermal diffusivity data for UM3. □, Heating; ▲, cooling.

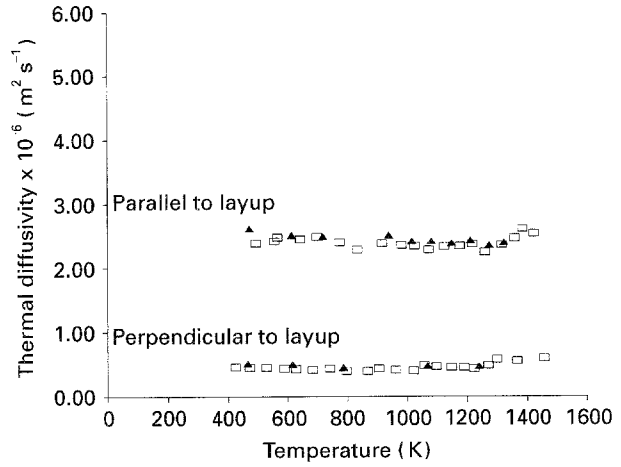

Figure 18 Thermal diffusivity data for UM4. □, Heating; ▲, Cooling.

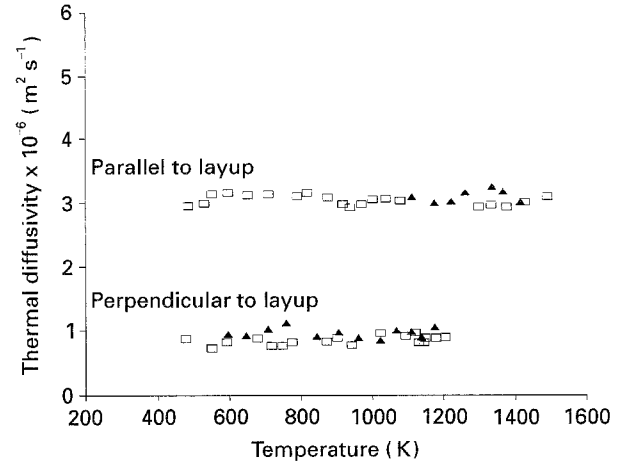

Figure 19 Thermal diffusivity data for UM5. □, Heating; ▲, cooling.

The graphs of diffusivity against temperature for samples UM2–5 are given in Figs 16–19, respectively. For all these graphs, the values for the heating and cooling curves for one direction both remain constant and equal over the whole temperature range. The values for UM5 perpendicular to the layup are limited to 1000 °C because of equipment malfunction. The average diffusivity values are listed in Table V. In each case the

TABLE V Average thermal diffusivities for the 2D composites

	Diffusivity normal to fibre layup (10^{-6} m^2 s^{-1})	Diffusivity in plane of fibre layup (10^{-6} m^2 s^{-1})
UM2	1.2	3.6
UM3	1.0	2.8
UM4	0.5	2.4
UM5	0.9	3.1

in-plane thermal diffusivity is much higher than the diffusivity normal to the plane of the weaves by a factor of 3–4 times.

Since the diffusivity curves show little variation with temperature, their conductivities will all follow the specific heat curve and show the same trend with temperature as the conductivity curve for UM1. The conductivity, or diffusivity, within the plane of a bidirectional fibre-reinforced system (λ_{2D}) is composed of two components: parallel and perpendicular to the fibres. Hence, if the fibre count is the same in both cross-ply directions of the 0°/90° laminate, the in-plane composite conductivity may be obtained from Equation 7

$$\lambda_{2D} = \frac{1}{2}\lambda_{1D\parallel} + \frac{1}{2}\lambda_{1D\perp} \quad (7)$$

where $\lambda_{1D\parallel}$ and $\lambda_{1D\perp}$ are the conductivities of the unidirectional composite in the longitudinal and transverse directions, respectively [26]. This assumes that the generic shape of the porosity is similar in the one and 2D composites. It is important, however, to realize that the terms in Equation 6 need to be re-evaluated for the bidirectional composite because the fibre volume fractions and porosity levels will be different. In order to do this, however, the exact geometry of the porosity needs to be characterized [26], and this is not practical. For the 2D composites the porosity levels are higher than for the 1D composite by a factor of more than two, and the fibre volume fractions slightly lower. Nevertheless, the conductivity or diffusivity is intermediate between that of the 1D parallel and perpendicular directions and an average value of 3.0×10^{-6} m^2 s^{-1} is obtained for the 2D composites.

For the bidirectional composites in the direction perpendicular to the weaves, if their porosity levels were similar, the diffusivities of the 2D composites should be similar to that for the unidirectional composite perpendicular to the fibre axis. A higher porosity level should result in a lower diffusivity and this trend is seen in the results in Table V.

4. Conclusion

Thermal expansion data and thermal conductivity data have been measured for a unidirectional and four bidirectional carbon fibre/SiC matrix composites. The results have been found to be entirely consistent with the microstructures caused by the filament-winding process and the polymer pyrolysis. For the unidirectional composite, the thermal expansion parallel to

the fibres has been found to be in reasonable agreement with that for pure silicon carbide. A conductivity curve for the matrix has been calculated using thermal transport theory and is found to rise over the temperature range used.

Acknowledgements

The authors wish to thank Dornier GmbH for the material used in this study; also the staff of Dornier GmBH, especially Dr. W. Vogel for helpful discussions. The project was funded through CEC under Brite-Euram.

References

1. P. LAMICQ, G. A. BERNHARDT, M. M. DAUCHIER and J. MACÉ, *Bull. Amer. Ceram. Soc.* **65** (1986) 336.
2. K. OKAMURA, *Composites* **18** (1987) 107.
3. W. D. VOGEL and U. SPELZ, *Ceram. Trans.* **51** (1995) 255.
4. J. T. MOTTRAM and R. TAYLOR, in "Encyclopedia of composites", Vol. 5, edited by S. M. Lee (VCH, New York, 1991) p. 476.
5. A. J. WHITTAKER, R. TAYLOR and H. TAWIL, *Proc. Roy. Soc. Lond. A* **430** (1990) 167.
6. H. TAWIL, L. D. BENTSEN, S. BASKARAN, and D. P. H. HASSELMANN, *J. Mater. Sci.* **20** (1985) 3201.
7. R. TAYLOR, J. R. BRANDON and V. PIDDOCK, *Brit. Ceram. Trans.* **92** (1993) 97.
8. H. IZAWA, Y. MIYAJI and Y. YAMAMOTO, *Taikubutsu* **41** (1989) 47.
9. E. SCAFÈ, G. GRILLO, L. FABBRI and V. VITTORI, *Ceram. Eng. Sci. Proc.* **13** (1992) 918.
10. Y. WANG, M. SASAKI, T. HIRAI, *J. Mater. Sci.* **26** (1991) 5495.
11. J. SEMEN and J. G. LOOP, *Ceram. Engng. Sci. Proc.* **11** (1990) 1387.
12. W. J. PARKER, R. J. JENKINS, C. P. BUTLER and G. L. ABBOTT, *J. Appl. Phys.* **32** (1961) 1670.
13. R. TAYLOR, *J. Phys. E* **13** (1980) 1193.
14. A. M. LUC and D. L. BALAGEAS, *High Temp.–High Press.* **16** (1984) 209.
15. R. E. TAYLOR and B. M. KELSIC, *J. Heat Trans.* **108** (1986) 161.
16. Y. S. TOULOUKIAN, R. K. KIRBY, R. E. TAYLOR and T. Y. R. LEE, in "Thermophysical properties of matter", Vol. 13 (Plenum, NY, 1977) p. 873.
17. J. F. VILLENEUVE, R. NASLAIN, R. FOURMEAUX and J. SEVELY, *Compos. Sci. Tech.* **49** (1993) 89.
18. L. HOLLIDAY and J. D. ROBINSON, in "Polymer engineering composites", edited by M. O. W. Richardson (Applied Science Publishers, London, 1977) Chapter 6.
19. D. K. HALE, *J. Mater. Sci.* **11** (1976) 2105.
20. B. YATES, M. J. OVERY, J. P. SARGENT, B. A. McCOLLA, D. M. KINGSTON-LEE, L. N. PHILIPS and K. F. ROYAN, *J. Mater. Sci.* **13** (1978) 433.
21. R. A. SCHAPERY, *J. Compos. Mater.* **2** (1968) 380.
22. J. F. LYNCH, C. G. RUDERER and W. H. DUCKWORTH, in "Engineering properties of selected ceramic materials" (American Ceramic Society, Ohio, 1966) 5.2.3-1.
23. Toray Company publicity literature.
24. R. TAYLOR, in "Encyclopedia of composites", Vol. 5, edited by S. M. Lee (VCH, New York, 1991) p. 530.
25. Y. S. TOULOUKIAN and E. H. BUYCO, in "Thermophysical properties of matter", Vol. 5 (Plenum, NY, 1970) p. 448.
26. R. TAYLOR, S. P. TURNER and K. GARNER, *High Temp.–High Press.* **25** (1993) 443.

Received 8 November 1994
and accepted 15 March 1995